CrossMark

Brain effective connectivity during motor-imagery and execution following stroke and rehabilitation

Sahil Bajaj[a,*], Andrew J. Butler[b,c,d], Daniel Drake[b], Mukesh Dhamala[a,d,e]

[a] Department of Physics and Astronomy, Georgia State University, Atlanta, GA, USA
[b] Byrdine F. Lewis School of Nursing & Health Professions, Georgia State University, Atlanta, GA, USA
[c] Department of Veteran's Affairs, Atlanta Rehabilitation Research and Development Center of Excellence, Decatur, GA, USA
[d] Neuroscience Institute, Georgia State University, Atlanta, GA, USA
[e] Center for Nano-Optics, Center for Behavioral Neuroscience, Center for Diagnostics and Therapeutics, Georgia State University, Atlanta, GA, USA

ARTICLE INFO

ABSTRACT

Brain areas within the motor system interact directly or indirectly during motor-imagery and motor-execution tasks. These interactions and their functionality can change following stroke and recovery. How brain network interactions reorganize and recover their functionality during recovery and treatment following stroke are not well understood. To contribute to answering these questions, we recorded blood oxygenation-level dependent (BOLD) functional magnetic resonance imaging (fMRI) signals from 10 stroke survivors and evaluated dynamical causal modeling (DCM)-based effective connectivity among three motor areas: primary motor cortex (M1), pre-motor cortex (PMC) and supplementary motor area (SMA), during motor-imagery and motor-execution tasks. We compared the connectivity between affected and unaffected hemispheres before and after mental practice and combined mental practice and physical therapy as treatments. The treatment (intervention) period varied in length between 14 to 51 days but all patients received the same dose of 60 h of treatment. Using Bayesian model selection (BMS) approach in the DCM approach, we found that, after intervention, the same network dominated during motor-imagery and motor-execution tasks but modulatory parameters suggested a suppressive influence of SM A on M1 during the motor-imagery task whereas the influence of SM A on M1 was unrestricted during the motor-execution task. We found that the intervention caused a reorganization of the network during both tasks for unaffected as well as for the affected hemisphere. Using Bayesian model averaging (BMA) approach, we found that the intervention improved the regional connectivity among the motor areas during both the tasks. The connectivity between PMC and M1 was stronger in motor-imagery tasks whereas the connectivity from PMC to M1, SM A to M1 dominated in motor-execution tasks. There was significant behavioral improvement (p = 0.001) in sensation and motor movements because of the intervention as reflected by behavioral Fugl-Meyer (FMA) measures, which were significantly correlated (p = 0.05) with a subset of connectivity. These findings suggest that PMC and M1 play a crucial role during motor-imagery as well as during motor-execution task. In addition, M1 causes more exchange of causal information among motor areas during a motor-execution task than during a motor-imagery task due to its interaction with SM A. This study expands our understanding of motor network involved during two different tasks, which are commonly used during rehabilitation following stroke. A clear understanding of the effective connectivity networks leads to a better treatment in helping stroke survivors regain motor ability.

* Corresponding author at: Department of Physics and Astronomy, Georgia State University, Suite 600, 25 Park Place, Atlanta, GA 30303, USA. Tel.: +1 404 413 6073; fax: +1 404 413 6025.
E-mail address: sahil.neuro@gmail.com (S. Bajaj).

1. Introduction

Numerous studies have investigated the characteristics of motor networks following stroke and it has been confirmed that stroke may cause a significant disturbance within the motor system due to direct tissue loss or damage of white matter fibers connecting different motor areas (Inman et al., 2012; James et al., 2009; Silasi and Murphy, 2014; Turken et al., 2008). This may result in temporary or permanent

physical disability among stroke survivors. Statistics published by The American Stroke Association and National Stroke Association confirms the importance of investigations related to stroke and interventions to promote recovery following stroke. Therefore, it is essential that we understand the detailed mechanism of reorganization of motor networks following stroke. It is also crucial to understand the effect of intervention on disturbed motor network as motor function is regained.

Motor-imagery and motor-execution tasks have been used to study motor recovery in people following stroke (Butler and Page, 2006; Lehéricy et al., 2004; Mintzopoulos et al., 2009; Sharma et al., 2006). Previous studies have investigated the effects of stroke on motor networks (Confalonieri et al., 2012; James et al., 2009; Jiang et al., 2013; Sharma et al., 2009) but there are little data on the effects of interventions on motor behavior and motor network interactions. Here, by using a dynamical causal modeling (DCM) approach (Friston et al., 2013; Friston et al., 2003; Valdes-Sosa et al., 2011), we investigated effective connectivity among three motor areas: the primary motor cortex (M1), the pre-motor cortex (PMC) and the supplementary motor area (SMA), which are known to interact during motor-execution and imagery tasks.

Mental practice (MP) and physical therapy (PT) are used frequently to improve motor function for people recovering from stroke. The primary goal of such treatments is to help patients regain motor strength or function that was completely or partially lost due to stroke. In the current study, we used either MP or combination of MP and PT. MP is defined as use of internal simulation that originates by creating an experience, which can be auditory, visual, tactile or kinesthetic but without any overt movements (Butler and Page, 2006; Dickstein and Deutsch, 2007). PT involves actual physical exercise, which has been demonstrated to improve learning and restoration of lost skills in stroke survivors.

Several studies have reported that cortical activation during MP are identical to PT (Hale, 1982; Livesay and Samaras, 1998). In a study by Altschuler et al. (1999), a comparison was done between movements of the impaired and the healthy arm; they found that several patients regained function of their affected arm when they watched the reflection of their healthy arm moving in a mirror, which may be regarded as an MP task. Recently, a combination of MP and PT has emerged as an effective tool to improve and characterize brain functionality at various stages following stroke (Bajaj et al., 2015; Butler and Page, 2006). It has been mentioned that following intervention PMC develops functional interactions with ipsilesional M1 (Grefkes and Fink, 2014; Silasi and Murphy, 2014). Although the source of the neuronal change associated with these interventions remains unclear. There is debate as to whether an intervention promotes the promulgation of same neuronal population during the recovery period or the intervention recruits other neuronal populations to compensate for the role played by affected neurons. A few studies (Schaechter et al., 2002; Wittenberg et al., 2003) have shown that repetitive task performance may lead to an increase in motor-map size in the affected hemisphere and this might be associated with a shift in laterality of motor cortical activation from damaged to undamaged hemisphere.

Brain activation and effective connectivity have been extensively studied in healthy people using motor-imagery and motor-execution tasks. Motor-imagery tasks (mental rehearsal) can involve a representation of movements in the brain (Jeannerod, 1995; Solodkin et al., 2004). The extent and distribution of activations may differ in motor-imagery and motor-execution, but both motor imagery and motor execution tasks activate the network that involves the core motor areas: M1, SM A and PMC (Bajaj et al., 2014; Cordes et al., 2000; Gerardin et al., 2000; Grefkes et al., 2008; Kasess et al., 2008). These areas are known to be involved in planning, initiation and execution of motor commands. The roles of SM A and PMC have been reported repeatedly during motor-imagery as well as during motor-execution tasks. They send neuronal impulses to M1. Several studies on effective connectivity and directed functional connectivity have reported the interactions of these

areas within themselves as well as with areas such as: the basal ganglia, putamen, cerebellum, inferior and superior parietal lobule and other somatosensory areas (Gao et al., 2011; Grefkes et al., 2008; Rehme et al., 2013; Walsh et al., 2008). SM A, M1 and PMC are known to be anatomically connected (Pool et al., 2013; Walsh et al., 2008).

In the present study, our analysis of brain effective connectivity within motor network of stroke patients is based on dynamical network modeling (DCM) (Friston et al., 2003). We hypothesized that either MP or MP + PT would (i) strengthen the effective connectivity on the affected side of the motor cortical network as patients regain motor ability and (ii) reorganize the connectivity pattern in the contralesional hemisphere. We tested these hypotheses by formulating several models using DCM using ordinary differential equations and compared the exceedance probability of each model. Exceedance probability represents the degree of belief about a model having higher posterior probability than the remaining models (Wasserman, 2000). We also explored and compared the role of M1 in affected and unaffected hemispheres during motor-imagery and motor-execution tasks.

2. Materials and methods

2.1. Participants and pre-scan measures

We recorded fMRI data from 13 adult stroke survivors. Three subjects had more than 2 mm of translation or more than 1.5° of rotation about the three axes or their data following intervention was not recorded properly and were excluded from the analysis. Four (2 females, 2 males) of the remaining 10 participants (4 females, 6 males) had left hemiparesis resulting from infarct or hemorrhage located in the thalamus, basal ganglia, caudate and pontomedullary. The remaining six volunteers had right hemiparesis due to infarctions of the middle cerebral, pontine or internal carotid arteries (Supplementary Table 1) (Inman et al., 2012). The mean age of the participants was 60.10 ± 10.52 years. All the participants were independent in standing, toilet transfer, could maintain balance for at least 2 min with arm support and met the criterion of being at-least 18 years old. Upper extremity movement criteria included the ability to actively extend the affected wrist ≥20° and extend 2 fingers and thumb at least 10° with a motor activity log (MAL) score of less than 2.5 (Uswatte et al., 2006). Either MR imaging or computed tomography (CT) was used to confirm the stroke location (Supplementary Table 1). Average stroke latency was 11 months and ranged from 1 to 54 months. The Mini-Mental State Exam (MMSE) (Folstein et al., 1975), Fugl-Meyer Motor Assessments (FMA) (Fugl-Meyer et al., 1975) and MIQ-RS (movement imagery questionnaire-revised for stroke) (Gregg et al., 2010) were used to assess cognitive aspects of mental function, sensation and motor function, and motor-imagery (kinesthetic and visual) ability respectively (Supplementary Table 1). The MMSE consisted of two sets of questions; the first tested orientation, memory and attention whereas the second set tested the participant's ability to name, follow verbal and written commands, write a sentence spontaneously and copy a complex polygon. A maximum score of 30 is indicative of normal cognitive function. The FMA included a total of 33 items including: reflexes, volitional movement assessment, flexor synergy, extension synergy, movement combining synergies, movement out of synergy, normal reflex assessment, wrist movement, hand movement, co-ordination and speed, each with a scale from 0 to 2 (0 for no performance, 1 for partial performance and 2 for complete performance). The total possible score was 66 where a score of nearly 33 represents moderate impairment of the affected upper limb. The MIQ-RS assesses how well people are able to mentally perform movements and consisted of everyday movements e.g. bending, pushing, pulling and reaching for and grasping (Butler et al., 2012; Gregg et al., 2010). Participants rated the level of ease/difficulty on a 7-point scale from 1 = very hard to see/feel to 7 = very easy to see/feel (Confalonieri et al., 2012).

2.2. Tasks

All participants were instructed to lay supine in the scanner with both arms outstretched close to their body. A block-design paradigm was used to run the task, which consisted of four runs (Confalonieri et al., 2012). Each run consisted of three stimulation blocks with an alternate 30 s period of passive rest. During the motor-imagery task, participants were instructed: 1) To track a sinusoidal wave while imagining the movement of the fingers of unaffected hand, called 'imagine unaffected (IU)' task and 2) to repeat the same task but now imagining the movement of fingers of affected hand, called 'imagine affected (IA)' task. During the motor-execution task, participants were instructed: 1) To track the same sinusoidal wave by continuously pinching a force transducer between thumb and index finger of the unaffected hand, called 'pinch unaffected (PU)' task and 2) to repeat the task with affected hand, called 'pinch affected (PA)' task. By providing visual feedback to the participants, we made sure that the participants performed the task as accurately as possible. Stroke patients practiced the tasks outside the scanner as well. As reported previously by Confalonieri et al. (2012), the relative root mean squared error (RRMSE) was very close to zero, which suggested a good control of grip force modulation. Also, time spent within target range (TWR) close to 30 s suggested a normal level of accuracy on matching the target force and the coefficient of co-ordination (K_c) close to 1 reflected normal coordination of grip force.

Four stroke-survivors had an affected left hemisphere and 6 had an affected right hemisphere. We separated data for the left and the right hemisphere, resulting in 8 sets of data for each participant:

(a) *Motor-imagery — imagine unaffected* (IU): (1) Four participants have right hemisphere unaffected and (2) six have left hemisphere unaffected.
(b) *Motor-imagery — imagine affected* (IA): (3) Six participants have right hemisphere affected and (4) four have left hemisphere affected.
(c) *Motor-execution — pinch unaffected* (PU): (5) Four participants have right hemisphere unaffected and (6) six have left hemisphere unaffected.
(d) *Motor-execution — pinch affected* (PA): (7) Six participants have right hemisphere affected and (8) four have left hemisphere affected.

2.3. Imaging

MR imaging was done using a Siemens 3.0 T Magnetom Trio scanner (Siemens Medical Solutions, Malvern, PA, USA) with a standard quadrature head coil and with TR/TE/FA=2350 ms/28 ms/90°, 130 time points (~5 min each), resolution = 3 × 3 × 3 mm³ and 35 axial slices. An anatomical image of each participant was acquired using a 3D magnetization-prepared rapid acquisition gradient echo (MPRAGE) sequence which consisted of 176 sagittal slices of 1 mm-thickness (resolution = 1 × 1 mm, in-plane matrix = 256 × 256) with TR/TE/FA/inversion time of 2300 ms/3.02 ms/8°/1100 ms. All stroke survivors underwent two tasks based scanning sessions. The delay between the scanning sessions ranged from 14 to 51 days. The second session was executed following an intervention where all the stroke survivors underwent either mental practice (MP) therapy or combined mental practice and physical therapy (MP + PT).

2.4. Intervention details

Six participants were randomized to "mentally practice" a series of upper limb functional motor tasks for 4 h per day (8–30 min sessions), with the guidance of an audio tape, for a total of 60 h over 3 weeks. MP is the creation of an experience by the mind, which can be auditory, visual, tactile or kinesthetic representing movement without undertaking physical effort. Seven participants were randomized to undergo combined mental practice and physical therapy (MP + PT). The MP + PT

group underwent 15 days (4 h per day) of intensive one-on-one therapy, consisting of listening to the same MP tape for 60 min per day plus 3 h of physical therapy per day. Identical tapes were given to all participants and the six mental practice tasks did not change, but small details of the mental practice scenarios such as the type of drink or color/type of telephone one reached for were altered to enhance motivation and lessen boredom.

The MP consisted of imagining four basic MI tasks using the affected or unaffected hand. For instance, participants were asked: (1) to imagine brushing or combing their hair, (2) to imagine picking up and bringing different types of fruit to their mouth, (3) to imagine extending their arm to pick up a cup from a cabinet and place it on the counter and gently release it, and (4) to imagine cleaning the kitchen counter using a cloth.

The PT consisted of repetitive, task-oriented training of the more-impaired upper extremity for several hours a day (depending on the severity of the initial deficit). Task oriented training involved functionally based activities performed continuously for a period of 15–20 min (e.g. writing in a journal). In successive periods of task training, the spatial requirement of the activity, or other parameters (such as duration), were changed to require more demanding control of limb segments for task completion. Feedback about overall performance was provided at the end of the 15–20 min period. A large bank of tasks was created for use among participants. Frequent rest intervals were provided through the training session.

All sessions had identical contact durations and were monitored by a licensed rehabilitation specialist. The investigators were blind to group assignment. Following the three-week "training" period all participants underwent a second testing session recording both clinical and physiologic measures.

2.5. Data analysis

2.5.1. FMRI preprocessing

FMRI data were preprocessed by using SPM8 (Wellcome Trust Centre for Neuroimaging, London; http://www.fil.ion.ucl.ac.uk/spm/software/spm8/). The preprocessing steps involved slice time correction, realignment, normalization and smoothing. Motion correction to the first functional scan was performed within participant using a six-parameter rigid-body transformation. Six motion parameters (three translational and three rotational) were stored and used as nuisance covariates. The mean of the motion-corrected images was then coregistered to the individual structural image using a 12-parameter affine transformation. The images were then spatially normalized to the Montreal Neurological Institute (MNI) template (Mazziotta et al., 1995) by applying a 12-parameter affine transformation, followed by a nonlinear warping using basis functions (Ashburner and Friston, 1999). Images were subsequently smoothed with an 8-mm isotropic Gaussian kernel and the low-frequency drifts in signal were removed using a standard band-pass-filter with a 128 s cutoff.

2.5.2. Volumes of interest (VOIs)

We defined volumes of interest for three basic motor areas — the primary motor cortex (M1), the premotor cortex (PMC) and the supplementary motor area (SMA) in SPM8 using the first eigen-variate of activations within a sphere of 8 mm radius centered at (−33, −19, 52), (36, −18, 52), (−34, −1, 56), (35, 0, 55) and (0, −4, 65) in MNI coordinate system for left M1, right M1, left PMC, right PMC and bilateral SM A respectively. In accordance with literature (Parker Jones et al., 2013), VOIs were defined by extracting mean time-series from the same set of voxels across the participants for each VOI corresponding to each of the four conditions. For that, we avoided any statistical threshold on activity within areas of interest so that extracted and adjusted time-series data remain spatially identical across all the participants (Parker Jones et al., 2013). Along with some disadvantages e.g. condition independent noise, there are several advantages supporting the use of this technique. No participant was excluded from the DCM analysis even if

activation in the areas of interest did not reach a pre-defined threshold ($p < 0.01$). A requirement for DCM is that all three VOIs were defined subject-wise according to next local maximum for affected and unaffected hemispheres. The participant specific maxima were constrained to lie within twice the width of Gaussian smoothing kernel (Bajaj et al., 2013; Li et al., 2010).

2.5.3. Dynamical causal modeling (DCM)

DCM is a hypothesis-based technique, which aims to describe how observed fMRI responses are generated using a set of differential equations. DCM incorporates known effects of interest and assesses task-dependent as well as tasking independent interactions among a group of regions through a set of matrices, known as an endogenous connectivity matrix, A and a modulatory matrix, B respectively (Friston et al., 2003; Pool et al., 2013). DCM estimates three sets of parameters: (a) task independent endogenous connectivity (matrix A) among the regions representing influence without any external perturbation, (b) task dependent modulation affects (matrix B) representing changes in endogenous connection strength due to external perturbations and (c) direct influence of an external input to a region (matrix C). The underlying principle behind DCM is that it considers the brain as a non-linear dynamical system where inputs are known along with experimental perturbations (Friston et al., 2003). This principle makes DCM different and potentially more effective than other traditional computational approaches like Granger causality and structural equation modeling which assume interactions are linear without considering external inputs and/or perturbations (Büchel and Friston, 1997).

Basically, DCM infers two types of hypothesis based on a specific question of interest. Those two inference types will be described below.

(a) *Bayesian model selection (BMS) approach*: BMS infers on a model structure as a whole, which is done by defining and constructing a model space. Model space is usually a set of models, where each model defines specific endogenous connections that are modulated by experimental perturbations. The BMS procedure identifies the model that best explains how the data are generated by calculating the exceedance probability of each model (Penny et al., 2004; Stephan et al., 2009). Best model is chosen with the highest model exceedance probability. Recently, the group-level BMS approach has been revised by Rigoux et al. (2014). They extended the BMS approach by introducing the 'Bayesian omnibus risk (BOR)' factor, which measures the statistical risk while performing group-level BMS analysis. This approach compares the likelihood of apparent differences in model frequencies by comparing

'protected exceedance probabilities' of proposed models i.e. it quantifies the frequency of a model, above and beyond chance (Rigoux et al., 2014).

(b) *Bayesian model averaging (BMA) approach*: For computational efficiency, BMA employs Occam's window and discards all the models with probability ratio <0.05 compared to the optimal model (Penny et al., 2010; Stephan et al., 2010). It infers on each connection of the optimal model found from BMS by averaging over all the optimal models from all the participants. Various statistical tests like *t*-test and ANOVA are used to find significant connection strength.

For group level inferences, BMS and BMA can be employed by either using fixed-effects (FFX) analysis or random-effects analysis (RFX) depending upon whether the effect of interest (model structure or parameters) is a fixed or a random variable due to inter-subject variability (e.g. in case of patients) across the population (Kasess et al., 2010).

In the current DCM study, we proposed a basic motor network model (model 1, Fig. 1) consisting of three motor areas: M1, PMC and SM A with bidirectional endogenous connections among them all. This corresponds to endogenous connectivity matrix, A, which is based on previous anatomical references for these three areas (Boussaoud et al., 2005; Luppino et al., 1993; Pool et al., 2013; Rouiller et al., 1994; Sharma et al., 2009). This basic model was elaborated into 7 more different models depending upon which endogenous connections from SM A and PMC were modulated by the external experimental input (represented by the term 'TASK' in Fig. 1), which can be either of IU, IA, PU and PA. Thus, for each condition, we proposed 8 models for each hemisphere (affected and unaffected), which sum to 64 models (32 before intervention and 32 after intervention) for each participant and each hemisphere. All the models were defined and estimated using a bilinear approach (Friston et al., 2003). We attempted to keep the model space as simple as possible and avoided including any complex model in order to maintain the balance between accuracy and complexity (Dima et al., 2011; Stephan et al., 2010).

3. Results

3.1. Effective connectivity

3.1.1. Optimal model selection

Considering areas from both unaffected (left and right) and affected (left and right) hemispheres, we calculated exceedance probabilities of all eight pre-defined models (model 1–model 8) (Fig. 1) of bilinear
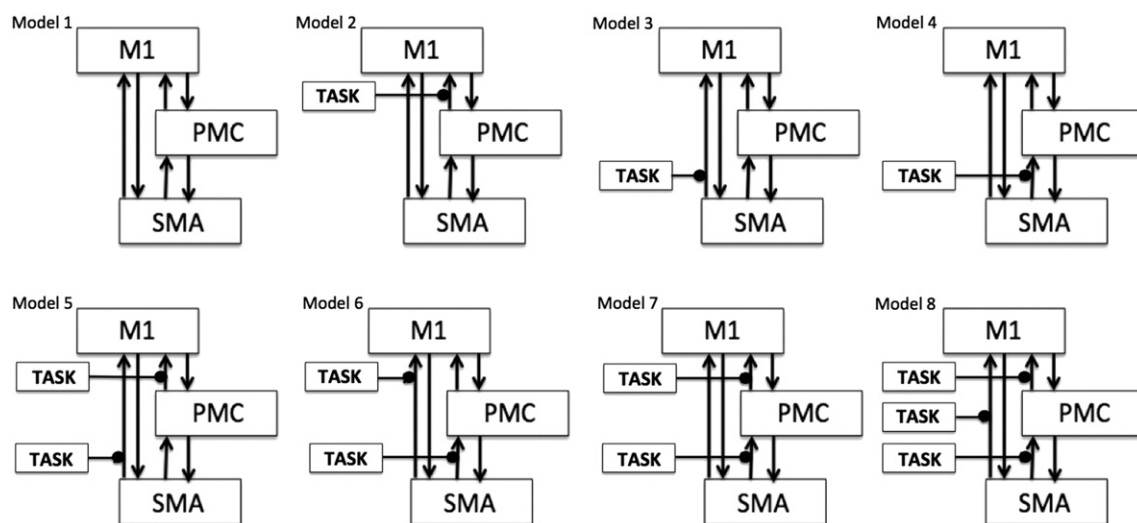
Fig. 1. Model space specification: Eight models (model 1–model 8) are specified constituting bilinear family for each condition. Here 'TASK' represents (1) imagine unaffected (IU), (2) imagine affected (IA), (3) pinch unaffected (PU) and (4) pinch affected (PA) condition for left (unaffected and affected) and right hemispheres (unaffected and affected).

Table 1

(a) Optimal model selection: The best model is selected by comparing model exceedance probabilities of top two models before and after intervention for each task condition. We found the same model (model 1) winning in case of imagery and execution task for unaffected hemisphere and same model (model 3) winning in case of imagery (IU) and execution task (PU and PA). We reported model 3 as winning model for imagery task, IA (after intervention). (b) Model 1 vs. model 3 model comparison and modulatory parameters from model 3. After intervention, comparing exceedance probabilities of model 1 and model 3, we found model 3 dominating over model 1 in case of IA-right and PU-left task conditions whereas model 1 was dominating over model 3 in case of PU-right task condition. The modulatory parameter for connection from SM A to M1 was negative for IA-right and positive for PU-left task condition. Here dominating models and their modulatory parameters (M.P.) are emphasized in bold.

(a) Optimal model selection

Condition	Hemisphere	Before intervention			After intervention			
		Optimal models			Optimal models			
		Model	E.P.	Optimal model (E.P.)	Model	E.P.	Optimal model (E.P.)	Optimal model (P.E.P.)
IU	Left	Model 1	0.45	Model 1 (0.45)	Model 1	0.44	Model 1 (0.44)	Model 1 (0.55)
		Model 4	0.17		Model 3	0.19		
	Right	Model 1	0.18		Model 1	0.26		
		Model 2	0.42		Model 6	0.32		
IA	Left	Model 4	0.18	Model 7 (0.43)	Model 3	0.35	Model 3 (0.35)	Model 3 (0.31)
		Model 7	0.43		Model 4	0.18		
	Right	Model 1	0.26		Model 2	0.27		
		Model 4	0.36		Model 7	0.19		
PU	Left	Model 3	0.26	Model 3 (0.39)	Model 3	0.22	Model 1 (0.31)	Model 1 (0.24)
		Model 6	0.28		Model 5	0.27		Model 5 (0.24)
	Right	Model 2	0.11		Model 1	0.31		
		Model 3	0.39		Model 4	0.29		
PA	Left	Model 1	0.17	Model 1 (0.31)	Model 1	0.23	Model 1 (0.37)	Model 1 (0.32)
		Model 7	0.28		Model 2	0.26		
	Right	Model 1	0.31		Model 1	0.37		
		Model 8	0.23		Model 3	0.28		

(b) Model 1 vs. model 3 comparison and modulatory parameters (M.P.) (in Hz) from model 3

Condition	Hemisphere	After intervention				
		Model	E.P.	Optimal model (E.P.)	M.P. (mean ± S.D.) for SMA to M1	Optimal model (P.E.P.)
IU	Left	Model 1	0.51	None	N.A.	None
		Model 3	0.49			
	Right	Model 1	0.49			
		Model 3	0.51			
IA	Left	Model 1	0.51	None	N.A.	Model 3 (0.57)
		Model 3	0.49			
	Right	Model 1	0.22	Model 3 (0.78)	−0.0111 ± 0.0045	
		Model 3	0.78			
PU	Left	Model 1	0.07	Model 3 (0.93)	0.0254 ± 0.0048	Model 3 (0.57)
		Model 3	0.93			
	Right	Model 1	0.82	Model 1 (0.82)	N.A.	
		Model 3	0.18			
PA	Left	Model 1	0.50	None	N.A.	None
		Model 3	0.50			
	Right	Model 1	0.50			
		Model 3	0.50			

IU: Imagine unaffected; IA: imagine affected; PU: pinch unaffected; PA: pinch affected; E.P.: exceedance probability; P.E.P.: protected exceedance probability; M.P.: modulatory parameter; S.D.: standard deviation; N.A.: not applicable.

family using BMS RFX criterion. Exceedance probabilities of first two optimal models for each condition before and after intervention are shown in Table 1(a).

(a) Motor-imagery: before and after intervention
Unaffected hemisphere: For the left hemisphere, we found the same model 1 as the optimal model before and after intervention (Supplementary Fig. 1A–B). For the right hemisphere, model 2 was the optimal model before intervention (Supplementary Fig. 1C) and model 6 was the optimal model after intervention (Supplementary Fig. 1D). Hence for IU condition, overall we found model 1 was the optimal model before as well as after the intervention (Table 1(a)).
Affected hemisphere: For the left hemisphere, we found model 7 was the optimal model before intervention (Supplementary Fig. 2A) and model 3 was the optimal model after intervention (Supplementary Fig. 2B). For the right hemisphere, model 4 was the optimal model before intervention (Supplementary Fig. 2C) and model 2 was the optimal model after intervention (Supplementary Fig. 2D). Hence for IA condition, overall we found model 7 was the optimal model before intervention and model 3 was the optimal model after intervention (Table 1(a)).

(b) Motor-execution: before and after intervention
Unaffected hemisphere: For the left hemisphere, we found model 6 was the optimal model before intervention (Supplementary Fig. 3A) and model 5 was the optimal model after intervention (Supplementary Fig. 3B). For the right hemisphere, model 3 was the optimal model before intervention (Supplementary Fig. 3C) and model 1 was the optimal model after intervention (Supplementary Fig. 3D). Hence for PU condition, overall we found model 3 was the optimal model before intervention and model 1 was the optimal model after intervention (Table 1(a)).
Affected hemisphere: For the left hemisphere, we found model 7 was the optimal model before intervention (Supplementary Fig. 4A) and model 2 was the optimal model after intervention (Supplementary Fig. 4B). For the right hemisphere, model 1 was the optimal model before as well as after intervention (Supplementary Fig. 4C–D). Hence for PA condition, overall we found model 1 was the optimal before and after intervention in the affected hemisphere (Table 1(a)).

Further, we made sure that the optimal model after intervention for each of the above conditions was consistent with the optimal model found from protected exceedance probabilities calculated by combining left and right hemispheres for corresponding conditions (Table 1(a)).

(c) Motor-imagery vs. motor-execution: after intervention
Comparing exceedance probabilities of optimal models (Table 1(a)) after intervention for motor-imagery and motor-execution, we found the same optimal model (model 1) for IU, PU and PA conditions and model 3 for IA condition. Since none of the models were clearly winning with an appreciable probability value, we compared models 1 and 3 for each condition after intervention (Table 1(b)). We found that model 3 was the dominant model over model 1 in case of IA-right and PU-left task conditions but model 1 was the dominant model over model 3 for PU-right task condition. Again, we made sure that the optimal model after intervention for each condition was consistent with the optimal model found from protected exceedance probabilities calculated by combining left and right hemispheres for corresponding conditions (Table 1(b)).
The modulatory parameter for connections from SM A to M1 was negative for IA-right and positive for PU-left task condition (Fig. 2). For other task conditions where we did not find any model clearly winning over the other, we found either highly negative or very weak positive modulation from SM A to M1 during the imagination task but strong positive modulation from SM A to M1 during the execution task.

3.1.2. Bayesian parameters and significance tests

Using the BMA approach, we calculated the endogenous and modulatory connection strength parameters (in Hz) by averaging over the optimal models of each participant and for each condition, followed by significance tests. For each connection, the mean of these effective connectivity measures along with standard deviation (SD) and p-value (using one sample t-test) for the left and right hemispheres, before and after intervention for unaffected and affected hemisphere are shown in Table 2 for the motor-imagery task and in Table 3 for the motor-execution tasks. Significant connections are marked with an asterisk in Figs. 3 and 4. For each condition,
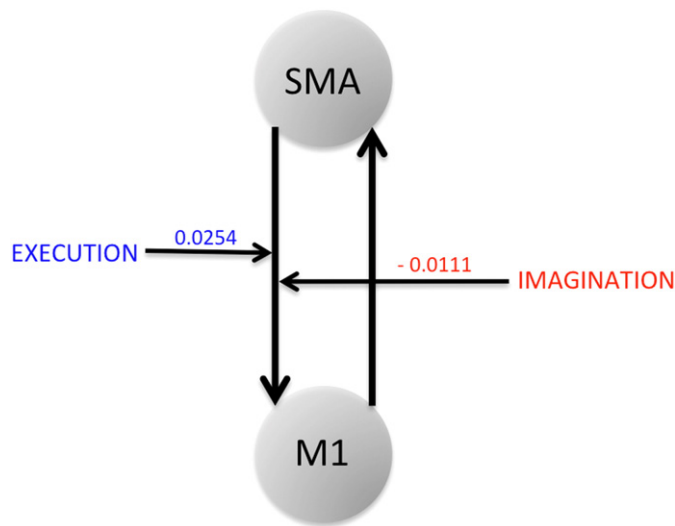
Fig. 2. Modulatory parameters from optimal model selection: SM A to M1 connection is positively modulated during motor-execution (ME) whereas the same connection is negatively modulated during motor-imagery (MI). Here optimal model for ME has model exceedance probability of 0.93 whereas optimal model for MI has model exceedance probability of 0.78.

Table 2
Effective connectivity measures: Endogenous and modulatory connectivity parameters for imagine unaffected (IU) and imagine affected (IA) tasks before and after the intervention.

Connection type	Mean (IU, IA)	SD (IU, IA)	p-Value (IU, IA)
Left hemisphere			
Before intervention			
Endogenous parameters			
PMC → M1	0.144, 0.128	0.021, 0.013	0.051, 0.006*
SMA → M1	0.036, 0.101	0.020, 0.010	0.507, 0.153
M1 → PMC	0.158, 0.140	0.021, 0.011	0.037*, 0.008*
SMA → PMC	0.108, 0.190	0.017, 0.010	0.337, 0.033*
M1 → SMA	0.074, 0.179	0.022, 0.013	0.315, 0.089
PMC → SMA	0.185, 0.258	0.019, 0.014	0.089, 0.026*
Modulatory parameters			
PMC → M1	−0.005, 0.015	0.018, 0.004	0.721, 0.259
SMA → M1	−0.009, 0.000	0.024, 0.000	0.480, N.A.
SMA → PMC	0.006, 0.038	0.005, 0.004	0.523, 0.145
After intervention			
Endogenous parameters			
PMC → M1	0.166, 0.183	0.013, 0.013	0.012*, 0.009*
SMA → M1	0.109, 0.137	0.011, 0.010	0.016*, 0.026*
M1 → PMC	0.190, 0.185	0.014, 0.012	0.030*, 0.004*
SMA → PMC	0.060, 0.165	0.011, 0.010	0.327, 0.036*
M1 → SMA	0.174, 0.186	0.014, 0.013	0.023*, 0.066
PMC → SMA	0.084, 0.197	0.014, 0.014	0.278, 0.018*
Modulatory parameters			
PMC → M1	0.021, 0.043	0.006, 0.004	0.227, 0.391
SMA → M1	0.007, −0.006	0.006, 0.005	0.177, 0.334
SMA → PMC	−0.011, 0.002	0.004, 0.001	0.247, 0.391
Right hemisphere			
Before intervention			
Endogenous parameters			
PMC → M1	0.110, 0.101	0.014, 0.019	0.009*, 0.190
SMA → M1	0.150, 0.099	0.012, 0.018	0.012*, 0.055
M1 → PMC	0.122, 0.105	0.010, 0.019	0.030*, 0.156
SMA → PMC	0.234, 0.189	0.011, 0.017	0.004*, 0.003*
M1 → SMA	0.180, 0.113	0.011, 0.018	0.024*, 0.080
PMC → SMA	0.270, 0.248	0.013, 0.017	0.001*, 0.000*
Modulatory parameters			
PMC → M1	0.009, −0.000	0.005, 0.001	0.564, 0.363
SMA → M1	0.000, −0.004	0.000, 0.004	N.A., 0.518
SMA → PMC	0.016, 0.011	0.002, 0.005	0.391, 0.053
After intervention			
Endogenous parameters			
PMC → M1	0.148, 0.115	0.010, 0.016	0.042*, 0.019*
SMA → M1	0.128, 0.080	0.009, 0.015	0.014*, 0.178
M1 → PMC	0.152, 0.115	0.010, 0.011	0.017*, 0.020*
SMA → PMC	0.177, 0.173	0.010, 0.012	0.031*, 0.017*
M1 → SMA	0.178, 0.067	0.010, 0.011	0.002*, 0.453
PMC → SMA	0.226, 0.183	0.010, 0.013	0.003*, 0.032*
Modulatory parameters			
PMC → M1	−0.000, 0.039	0.010, 0.064	0.391, 0.319
SMA → M1	0.003, 0.017	0.013, 0.065	0.827, 0.355
SMA → PMC	0.030, 0.003	0.011, 0.005	0.184, 0.795

S.D.: Standard deviation; N.A.: not applicable.
* $p < 0.05$.

we did not consider non-significant connections of both left and right hemispheres.

(a) Motor-imagery: before and after intervention
Before intervention: We found that the connection from M1 to PMC was the only significant connection ($p < 0.05$) for IU (Fig. 3A) and the connection between SM A and PMC was the only significant connection ($p < 0.05$) for IA (Fig. 3B).
After intervention: We found significant bidirectional connections between PMC and M1, and between SM A and M1 ($p < 0.05$) for IU (Fig. 3C) and significant bidirectional connection between SM A and PMC, along with connection between PMC and M1 ($p < 0.05$) for IA (Fig. 3D).

(b) Motor-execution: before and after intervention
Before intervention: We found that the only significant connection was between M1 and PMC ($p < 0.05$) for PU (Fig. 4A)

Table 3

Effective connectivity measures: Endogenous and modulatory connectivity parameters for pinch unaffected (PU) and pinch affected (PA) tasks before and after the intervention.

Connection type	Mean (PU, PA)	SD (PU, PA)	p-Value (PU, PA)
Left hemisphere			
Before intervention			
Endogenous parameters			
PMC → M1	0.215, 0.173	0.012, 0.027	0.000[*], 0.028[*]
SMA → M1	0.002, 0.105	0.011, 0.027	0.978, 0.198
M1 → PMC	0.238, 0.142	0.013, 0.028	0.001[*], 0.013[*]
SMA → PMC	0.117, 0.222	0.011, 0.027	0.222, 0.010[*]
M1 → SMA	0.005, 0.143	0.011, 0.026	0.948, 0.037[*]
PMC → SMA	0.180, 0.239	0.011, 0.028	0.091, 0.002[*]
Modulatory parameters			
PMC → M1	0.004, 0.005	0.027, 0.121	0.336, 0.345
SMA → M1	−0.008, −0.002	0.021, 0.121	0.313, 0.078
SMA → PMC	0.000, 0.010	0.006, 0.020	0.948, 0.357
After intervention			
Endogenous parameters			
PMC → M1	0.216, 0.192	0.013, 0.027	0.001[*], 0.009[*]
SMA → M1	0.037, 0.173	0.012, 0.026	0.037[*], 0.015[*]
M1 → PMC	0.265, 0.217	0.012, 0.027	0.265, 0.018[*]
SMA → PMC	0.132, 0.111	0.010, 0.026	0.132, 0.227
M1 → SMA	0.075, 0.235	0.012, 0.026	0.075, 0.003[*]
PMC → SMA	0.184, 0.108	0.013, 0.025	0.184, 0.354
Modulatory parameters			
PMC → M1	0.013, 0.005	0.017, 0.039	0.059, 0.170
SMA → M1	0.013, 0.003	0.020, 0.029	0.258, 0.245
SMA → PMC	0.006, 0.000	0.005, 0.004	0.434, 0.423
Right hemisphere			
Before intervention			
Endogenous parameters			
PMC → M1	0.171, 0.180	0.020, 0.023	0.003[*], 0.000[*]
SMA → M1	0.090, 0.153	0.017, 0.018	0.005[*], 0.000[*]
M1 → PMC	0.185, 0.176	0.016, 0.020	0.011[*], 0.001[*]
SMA → PMC	0.236, 0.162	0.015, 0.016	0.002[*], 0.001[*]
M1 → SMA	0.116, 0.179	0.020, 0.021	0.006[*], 0.000[*]
PMC → SMA	0.259, 0.196	0.020, 0.022	0.001[*], 0.000[*]
Modulatory parameters			
PMC → M1	0.020, 0.008	0.067, 0.092	0.205, 0.240
SMA → M1	−0.012, 0.012	0.073, 0.077	0.466, 0.127
SMA → PMC	0.004, 0.001	0.005, 0.006	0.391, 0.924
After intervention			
Endogenous parameters			
PMC → M1	0.158, 0.184	0.012, 0.022	0.003[*], 0.000[*]
SMA → M1	0.171, 0.130	0.010, 0.018	0.038[*], 0.003[*]
M1 → PMC	0.144, 0.165	0.011, 0.017	0.003[*], 0.000[*]
SMA → PMC	0.161, 0.173	0.010, 0.016	0.110, 0.000[*]
M1 → SMA	0.204, 0.174	0.012, 0.018	0.060, 0.002[*]
PMC → SMA	0.211, 0.258	0.013, 0.021	0.112, 0.000[*]
Modulatory parameters			
PMC → M1	0.017, 0.011	0.016, 0.043	0.391, 0.223
SMA → M1	0.006, 0.002	0.012, 0.043	0.391, 0.326
SMA → PMC	−0.006, 0.011	0.003, 0.005	0.449, 0.222

S.D.: Standard deviation.

[*] p < 0.05.

and all the connections except from SM A to M1 were significant (p < 0.05) for PA (Fig. 4B).

After intervention: We found two significant connections: one from PMC and M1, and other from SM A to M1 (p < 0.05) for PU (Fig. 4C) and all the connections were significant except between SM A and PMC (p < 0.05) for PA (Fig. 4D).

(c) Motor-imagery vs. motor-execution: after intervention
We eliminated the connections that were not common between the unaffected and affected hemisphere after intervention. We found that the strongest connection during the motor imagery task was a bidirectional connection between PMC and M1 (Fig. 3C–D). Similarly, there were two connections, one from PMC to M1 and other from SM A to M1 that were the strongest for the motor-execution task (Fig. 4C–D). These connections are indicated with blue colored arrows in Figs. 3 and 4.

3.2. Brain and behavior correlation

We recorded FMA scores for all the stroke-survivors before and after intervention. Using paired t-test; we found that FMA scores were significantly higher (sample size = 10; p = 0.001) when the participants underwent a session of intervention (Fig. 5). We also calculated the difference between FMA scores and endogenous connectivity measures before and after intervention. We found a significant linear correlation between the two for the connection from PMC to SM A (correlation coefficient, r = 0.94, p = 0.05) for the left affected hemisphere during motor-imagery task whereas the correlation for the connection from SM A to PMC under the same condition tended towards significant value (correlation coefficient, r = 0.88). Also, the correlation for connection from SM A to PMC for left unaffected hemisphere (correlation coefficient, r = 0.69) and from PMC to M1 for left affected hemisphere (correlation coefficient, r = 0.87) during the motor-execution task tended towards significance.

4. Discussion

In this study, we used a dynamical causal modeling approach on task-based fMRI data to describe the effect of stroke and intervention on the brain. We examined the effective connectivity among numerous cortical areas and found that, after intervention, the optimal models were identical between motor imagery and motor execution tasks for the unaffected hemisphere. Modulatory parameters showed a suppressive (negative) influence of SM A on M1 during the motor-imagery task and an unrestricted (positive) influence of SM A on M1 during the motor-execution task. We also found that for both the hemispheres, intervention caused a reorganization of connectivity patterns among these areas. Inter-regional effective connectivity measures showed that although PMC and M1 were both involved during motor imagery and execution tasks, M1 had a more crucial role along with SM A during the motor-execution task compared to the motor-imagery task. We also report that FMA scores were significantly higher following intervention and there was a significant linear correlation or a correlation which tended towards a significant value between difference in FMA scores and difference in endogenous connectivity measures following stroke and when the stroke-survivors underwent intervention. In this study, we used dynamical causal modeling approach to look at the effective connectivity from task-related fMRI data, but there are other approaches to study network interactions (Friston, 2011) including parametric Granger causality (Ding et al., 2006, 1975; Geweke, 1982; Granger, 1969) and nonparametric Granger causality (Dhamala, 2014; Dhamala et al., 2008a, 2008b; Hu and Liang, 2014; Hu and Liang, 2012).

4.1. Effective connectivity during motor-imagery and motor-execution

Our findings are consistent with several previous neuroimaging studies. Using the BMS approach we found that following an intervention the winning model showed substantial influence of SM A on M1 during motor-imagery as well as during a motor-execution task. Comparing modulatory parameters of both the tasks showed suppressive influence of SM A on M1 during the motor-imagination task and the influence appeared to strengthen the connection from SM A to M1 during the motor-execution task. This suggests that although there were common areas, which were shared between the two tasks, the activated networks differed. Similar findings have been reported that motor-imagination had negative and motor-execution had positive (opposite) effect on the connection from SM A to M1 (Gao et al., 2011; Grefkes et al., 2008; Kasess et al., 2008; Pool et al., 2013; Raffin et al., 2012; Westlake and Nagarajan, 2011; Xu et al., 2013). Absence of modulation from PMC to M1 by both tasks reflects weak effective connectivity
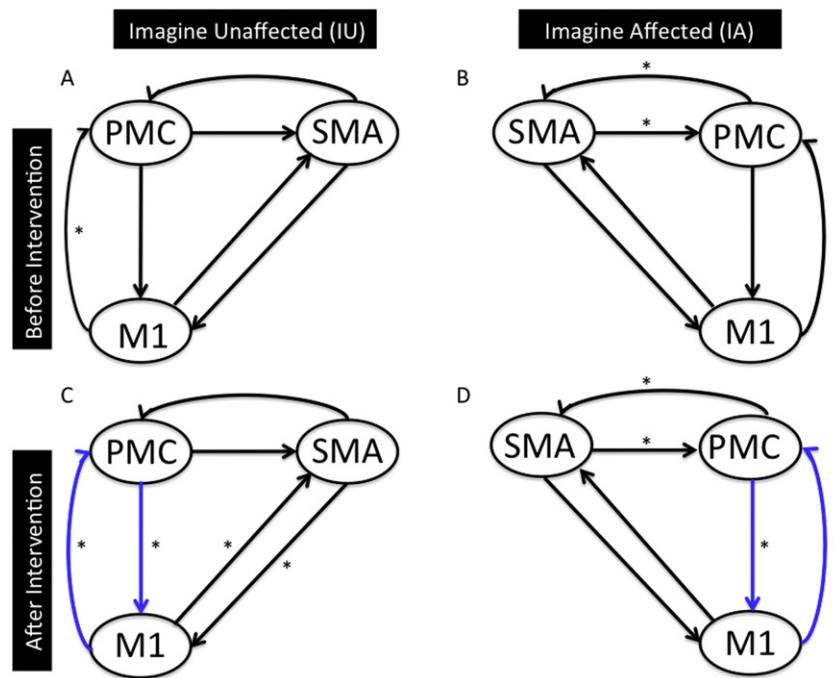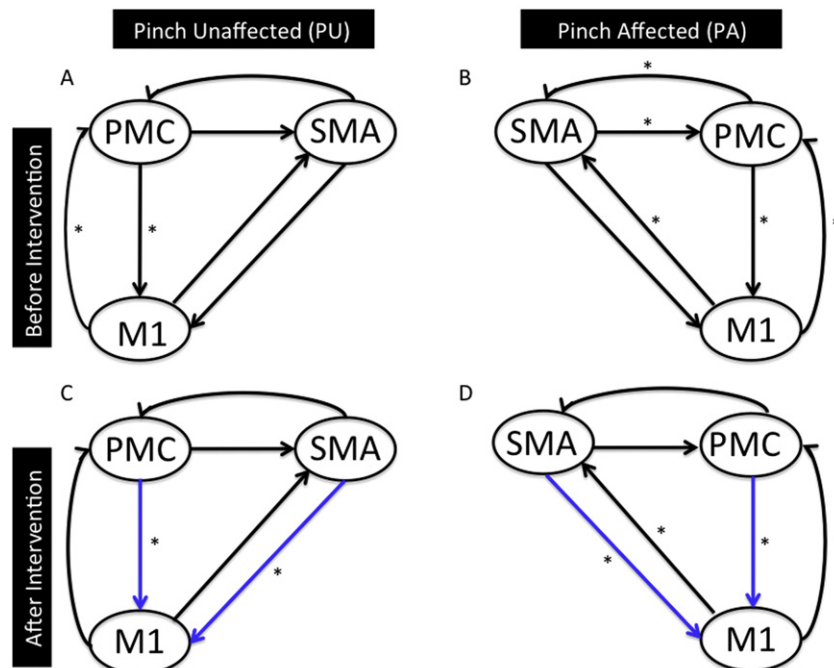
Fig. 3. Effective connectivity network for motor-imagery task: Endogenous connectivity for motor-imagery task before (A–B) and after (C–D) intervention is shown. Here significant connections represented by * (p < 0.05) are found using one sample t-test. Connections shown in blue color are common between IU (after intervention) and IA (after intervention).

between PMC and M1. This is consistent with a study by Solodkin and colleagues in 2004 (Solodkin et al., 2004). They reported that a decreased influence of PMC on M1 was accompanied by a stronger influence of SM A on M1 during mental simulation of movement. The inter-regional effective connectivity measures between SM A and M1 during motor-execution also suggest bidirectional influence between the two which is consistent with a study by Kasess et al. (2008), who used DCM, to demonstrate a suppressive influence exerted by SM A

on M1 with a subsequent feedback influence from M1 to SM A. They reported that SM A may inhibit activity of M1 and may be capable of sustaining activity for several seconds throughout the readiness prior to movement.

Using structural equation modeling, Solodkin and colleagues found motor-imagery and motor-execution tasks activate a basic motor network, yet volumes of activation differ for these two dissimilar tasks (Hanakawa et al., 2008; Solodkin et al., 2004). Using a conditional

Fig. 4. Effective connectivity network for motor-execution task: Endogenous connectivity for motor-execution task before (A–B) and after (C–D) intervention is shown. Here significant connections represented by * (p < 0.05) are found using one sample t-test. Connections shown in blue color are common between PU (after intervention) and PA (after intervention).
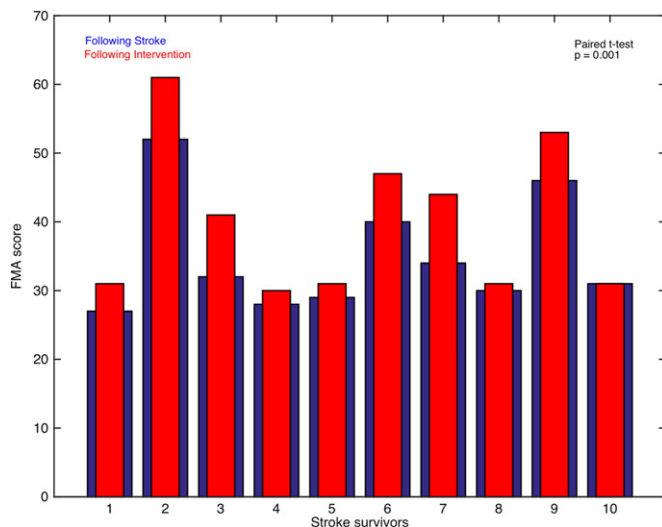
Fig. 5. FMA scores: The FMA scores for stroke-survivors following stroke (blue bars) and following intervention (red bars) are plotted.

Granger causality technique (Gao et al., 2011), it was shown that more causal information was exchanged during motor-execution than during motor-imagery. This may be due to some additional neuronal processes occurring because of direct execution of physical movements (Munzert et al., 2009). By calculating in-out causal flow, these investigators also found that in addition to inferior parietal lobule (IPL) and superior parietal lobule (SPL), dorsal PMC (dPMC) also acted as a causal source in motor-imagery and motor-execution tasks. This is consistent with our findings from the BMA parameters. We find that connectivity between PMC and M1 and from PMC to M1 is stronger during the motor-imagery and motor-execution tasks respectively, whereas there is additional significant connection from SM A to M1 during the motor-execution task. This is consistent with the canonical role of PMC in movement planning which is common between motor-imagery and motor-execution. From inter-regional connectivity measures, we found that PMC is more dominant during the motor-imagery task in comparison to the motor-execution task. This might be because kinesthetic motor-imagery has the capability to boost motor-evoked potentials at the level of premotor areas (Hanakawa et al., 2008; Li et al., 2004; Sharma et al., 2009). These findings confirmed that although there were overlapping motor areas during motor-imagery and motor-execution, the interaction between SM A and M1 caused more exchange of causal information within motor network during the motor-execution task.

4.2. Effect of intervention on effective connectivity

In the present study, BMS results reflect the reorganization of connectivity patterns following intervention. Although the degree of regaining motor skills varies from patient-to-patient depending on the location and extent of lesion (Silasi and Murphy, 2014), stroke patients manage to recover their motor ability. The degree to which motor ability is regained depends on the size of neuronal populations that are thought to reorganize during the intervention period, which may further depend on the intensity of post-stroke therapy. We reported that the intervention significantly improved FMA scores as well as the connectivity between specific cortical areas. We found that difference in FMA scores and connectivity measures before and after intervention follow a linear trend, especially for the connection from PMC to SM A. Previously, an increase in neural activity of M1, SM A, PMC and the superior parietal cortex in humans has been linked to greater improvement of hand motor function (Grefkes and Fink, 2014). It has also been shown that after injury, lateral PMC may play a significant role in

mediating the recovery process (McNeal et al., 2010). Using structural equation modeling, Sharma and colleagues (2009) found that coupling between PMC and SM A diminished in stroke patients and as motor function improved, the coupling between these areas along with ipsilesional PMC to M1 increased during motor-imagery task which could be due to enhancement of cortical–cortical interactions following intervention (Sharma et al., 2009). Our findings are consistent with the findings reported by Page et al. (2007). They reported that the mental practice improved scores on the Action Research Arm (ARA) test and Upper Extremity Fugl-Meyer Assessment (FMA) by an average of 7.81 and 6.72 after stroke. Although the mechanism behind recovery of motor skills is not well understood but a well-known notion behind this is that after an effective intervention, the unaffected brain areas undergo structural and functional remodeling and take over the function of affected brain areas by remapping the post functions (Brown et al., 2009; Mostany et al., 2010; Silasi and Murphy, 2014). In a study on adult squirrel monkeys by Nudo et al. (1996), it was reported that monkeys suffering from lesions to motor cortex, could use alternative brain areas to compensate for motor impairments. Arya et al. (2011) also suggested that motor recovery following rehabilitation could either be: (1) true motor recovery, which comes into play when alternative connections that are undamaged send commands to the same affected muscles to execute the motor commands or (2) compensatory motor recovery which involves sending neuronal commands to alternative but unaffected muscles (Krakauer, 2006). In our case, several other factors like task specification e.g. goal-oriented repetitive task practice and a proper environment during rehabilitation might have played significant roles to functionally reorganize the motor networks in order to regain motor ability (Arya et al., 2011; Davis, 2006). Task specification may also help engage brain areas that are adjacent to the affected areas (Nudo et al., 2000). Repetition of task-oriented training has been reported to be more effective (Page et al., 2007).

Limitations: The sample included stroke survivors with wide range of stroke latency. Individual behavioral and brain deficit differences following stroke may have added further variability to the endogenous and modulatory measures. Despite the variability and small sample size, our data showed a robust correlation between endogenous connectivity measures and behavioral measures.

In a larger pool of stroke patients, it may be possible to separate enough stroke patients by a narrow range of stroke intervals and similar stroke locations and examine these motor networks, which may provide results with even stronger brain–behavior correlation. We did not directly test the functional relevance of unaffected hemisphere for the changes in regions of the affected hemisphere. However, we found that the connectivity discovered in unaffected hemispheres helps to find the robust connectivity common across affected and unaffected hemispheres after the intervention.

5. Conclusions

In conclusion, the results of the current DCM study describe the disturbances caused in motor network following stroke. Findings reported in this study describe how different motor areas are reorganized after treatment. The roles of PMC and M1 have been specifically emphasized during motor-imagery and motor-execution tasks. The inter-regional and network level effective connectivity approaches show the importance of treatments like mental practice and physical therapy during motor recovery and in order to better understand the mechanism behind the recovery process.

Supplementary data to this article can be found online at http://dx.doi.org/10.1016/j.nicl.2015.06.006.

Conflicts of interest

All the authors declared no conflicts of interest.

Acknowledgments

References

Altschuler, E.L., Wisdom, S.B., Stone, L., et al., 1999. Rehabilitation of hemiparesis after stroke with a mirror. Lancet 353 (9169), 2035–2036. http://dx.doi.org/10.1016/S0140-6736(99)00920-410376620.

Arya, K.N., Pandian, S., Verma, R., et al., 2011. Movement therapy induced neural reorganization and motor recovery in stroke: a review. The. rev. 15 (4), 528–537. http://dx.doi.org/10.1016/j.jbmt.2011.01.02321943628.

Ashburner, J., Friston, K.J., 1999. Nonlinear spatial normalization using basis functions. Hum. Brain Mapp. 7 (4), 254–26610408769.

Bajaj, S., Butler, A.J., Drake, D., et al., 2015. Functional organization and restoration of the brain motor-execution network after stroke and rehabilitation. Front. Hum. Neurosci. 9, 173. http://dx.doi.org/10.3389/fnhum.2015.0017325870557.

Bajaj, S., Drake, D., Butler, A.J., et al., 2014. Oscillatory motor network activity during rest and movement: an fNIRS study. Front. Syst. Neurosci. 8, 13. http://dx.doi.org/10.3389/fnsys.2014.0001324550793.

Bajaj, S., Lamichhane, B., Adhikari, B.M., et al., 2013. Amygdala mediated connectivity in perceptual decision-making of emotional facial expressions. Brain Connect 3 (4), 386–397. http://dx.doi.org/10.1089/brain.2013.014523705655.

Boussaoud, D., Tanné-Gariépy, J., Wannier, T., et al., 2005. Callosal connections of dorsal versus ventral premotor areas in the macaque monkey: a multiple retrograde tracing study. B.M.C. Neurosci. 6, 67. http://dx.doi.org/10.1186/1471-2202-6-6716309550.

Brown, C.E., Aminoltejari, K., Erb, H., et al., 2009. In vivo voltage-sensitive dye imaging in adult mice reveals that somatosensory maps lost to stroke are replaced over weeks by new structural and functional circuits with prolonged modes of activation within both the peri-infarct zone and distant sites. J. Neurosci. 29 (6), 1719–1734. http://dx.doi.org/10.1523/JNEUROSCI.4249-08.200919211879.

Büchel, C., Friston, K.J., 1997. Modulation of connectivity in visual pathways by attention: cortical interactions evaluated with structural equation modelling and fMRI. Cereb. Cortex 7 (8), 768–7789408041.

Butler, A.J., Cazeaux, J., Fidler, A., et al., 2012. The movement imagery questionnaire-revised, second edition (MIQ-RS) is a reliable and valid tool for evaluating motor imagery in stroke populations. Evid. Based Complement. Alternat. Med. 2012, 497289. http://dx.doi.org/10.1155/2012/49728922474504.

Butler, A.J., Page, S.J., 2006. Mental practice with motor imagery: evidence for motor recovery and cortical reorganization after stroke. Arch. Phys. Med. Rehabil. 87 (12 Suppl 2), S2–11. http://dx.doi.org/10.1016/j.apmr.2006.08.32617140874.

Confalonieri, L., Pagnoni, G., Barsalou, L.W., et al., 2012. Brain activation in primary motor and somatosensory cortices during motor imagery correlates with motor imagery ability in stroke patients. I.S.R.N. Neuro. 2012, 613595. http://dx.doi.org/10.5402/2012/61359523378930.

Cordes, D., Haughton, V.M., Arfanakis, K., et al., 2000. Mapping functionally related regions of brain with functional connectivity MR imaging. A.J.N.R. Am. J. Neuroradiol. 21 (9), 1636–164411039342.

Davis, J.Z., 2006. Task selection and enriched environments: a functional upper extremity training program for stroke survivors. Top. Stroke Rehabil. 13 (3), 1–11. http://dx.doi.org/10.1310/D91V-2NEY-6FL5-26Y216987787.

Dhamala, M., 2014. Spectral interdependency methods. In: Jaeger, D., Jung, R. (Eds.), Encyclopedia of Computational Neuroscience. Springer, New York.

Dhamala, M., Rangarajan, G., Ding, M., 2008a. Analyzing information flow in brain networks with nonparametric Granger causality. Neuroimage 41 (2), 354–362. http://dx.doi.org/10.1016/j.neuroimage.2008.02.02018394927.

Dhamala, M., Rangarajan, G., Ding, M., 2008b. Estimating granger causality from Fourier and wavelet transforms of Time series data. Phys. Rev. Lett. 100 (1), 018701. http://dx.doi.org/10.1103/PhysRevLett.100.01870118232831.

Dickstein, R., Deutsch, J.E., 2007. Motor imagery in physical therapist practice. Phys. Ther. 87 (7), 942–953. http://dx.doi.org/10.2522/ptj.2006033117472948.

Dima, D., Stephan, K.E., Roiser, J.P., et al., 2011. Effective connectivity during processing of facial affect: evidence for multiple parallel pathways. J. Neurosci. 31 (40), 14378–14385. http://dx.doi.org/10.1523/JNEUROSCI.2400-11.201121976523.

Ding, M., Chen, Y., Bressler, S.L., 2006. Granger Causality: Basic Theory and Application to Neuroscience. Wiley, Wienheim.

Folstein, M.F., Folstein, S.E., McHugh, P.R., 1975. "Mini-mental state": a practical method for grading the cognitive state of patients for the clinician. J. Psychiatr. Res. 12 (3), 189–198.

Friston, K., Moran, R., Seth, A.K., 2013. Analysing connectivity with Granger causality and dynamic causal modelling. Curr. Opin. Neurobiol. 23 (2), 172–178. http://dx.doi.org/10.1016/j.conb.2012.11.01023265964.

Friston, K.J., 2011. Functional and effective connectivity: a review. Brain Connectivity 1 (1), 13–36. http://dx.doi.org/10.1089/brain.2011.0008.

Friston, K.J., Harrison, L., Penny, W., 2003. Dynamic causal modelling. Neuroimage 19 (4), 1273–1302. http://dx.doi.org/10.1016/S1053-8119(03)00202-712948688.

Fugl-Meyer, A.R., Jääskö, L., Leyman, I., et al., 1975. The post-stroke hemiplegic patient. 1. A method for evaluation of physical performance. Scand. J. Rehabil. Med. 7 (1), 13–311135616.

Gao, Q., Duan, X., Chen, H., 2011. Evaluation of effective connectivity of motor areas during motor imagery and execution using conditional Granger causality. Neuroimage 54 (2), 1280–1288. http://dx.doi.org/10.1016/j.neuroimage.2010.08.07120828626.

Gerardin, E., Sirigu, A., Lehéricy, S., et al., 2000. Partially overlapping neural networks for real and imagined hand movements. Cereb. Cortex 10 (11), 1093–110411053230.

Geweke, J., 1982. Measurement of linear dependence and feedback between multiple time series. J. Am. Statist. Assoc. 77 (378), 304–313.

Granger, C.W.J., 1969. Investigating causal relations by econometric models and cross-spectral methods. Econometrica 37 (3), 424–438. http://dx.doi.org/10.2307/1912791.

Grefkes, C., Eickhoff, S.B., Nowak, D.A., et al., 2008. Dynamic intra- and interhemispheric interactions during unilateral and bilateral hand movements assessed with fMRI and DCM. Neuroimage 41 (4), 1382–1394. http://dx.doi.org/10.1016/j.neuroimage.2008.03.04818486490.

Grefkes, C., Fink, G.R., 2014. Connectivity-based approaches in stroke and recovery of function. Lancet Neurol. 13 (2), 206–216. http://dx.doi.org/10.1016/S1474-4422(13)70264-324457190.

Gregg, M., Hall, C., Butler, A., 2010. The MIQ-RS: a suitable option for examining movement imagery ability. Evid. Based Complement. Alternat. Med. 7 (2), 249–257. http://dx.doi.org/10.1093/ecam/nem17018955294.

Hale, B.D., 1982. The effects of internal and external imagery on muscular and ocular concomitants. J. Sport Psychol. 4, 379–387.

Hanakawa, T., Dimyan, M.A., Hallett, M., 2008. Motor planning, imagery, and execution in the distributed motor network: a time-course study with functional MRI. Cereb. Cortex 18 (12), 2775–2788. http://dx.doi.org/10.1093/cercor/bhn03618359777.

Hu, M., Liang, H., 2014. A copula approach to assessing Granger causality. Neuroimage 100, 125–134. http://dx.doi.org/10.1016/j.neuroimage.2014.06.01324945669.

Hu, S., Liang, H., 2012. Causality analysis of neural connectivity: new tool and limitations of spectral Granger causality. Neurocomputing 76 (1), 44–47. http://dx.doi.org/10.1016/j.neucom.2010.10.017.

Inman, C.S., James, G.A., Hamann, S., et al., 2012. Altered resting-state effective connectivity of fronto-parietal motor control systems on the primary motor network following stroke. Neuroimage 59 (1), 227–237. http://dx.doi.org/10.1016/j.neuroimage.2011.07.08321839174.

James, G.A., Lu, Z.L., VanMeter, J.W., et al., 2009. Changes in resting state effective connectivity in the motor network following rehabilitation of upper extremity poststroke paresis. Top. Stroke Rehabil. 16 (4), 270–281. http://dx.doi.org/10.1310/tsr1604-27019740732.

Jeannerod, M., 1995. Mental imagery in the motor context. Neuropsychologia 33 (11), 1419–1432. http://dx.doi.org/10.1016/0028-3932(95)00073-C8584178.

Jiang, L., Xu, H., Yu, C., 2013. Brain connectivity plasticity in the motor network after ischemic stroke. Neural Plast. 2013, 924192. http://dx.doi.org/10.1155/2013/92419223738150.

Parker Jones, O., Seghier, M.L., Kawabata Duncan, K.J., et al., 2013. Auditory–motor interactions for the production of native and non-native speech. J. Neurosci. 33 (6), 2376–2387. http://dx.doi.org/10.1523/JNEUROSCI.3289-12.201323392667.

Kasess, C.H., Stephan, K.E., Weissenbacher, A., et al., 2010. Multi-subject analyses with dynamic causal modeling. Neuroimage 49 (4), 3065–3074. http://dx.doi.org/10.1016/j.neuroimage.2009.11.03719941963.

Kasess, C.H., Windischberger, C., Cunnington, R., et al., 2008. The suppressive influence of SMA on M1 in motor imagery revealed by fMRI and dynamic causal modeling. Neuroimage 40 (2), 828–837. http://dx.doi.org/10.1016/j.neuroimage.2007.11.04018234512.

Krakauer, J.W., 2006. Motor learning: its relevance to stroke recovery and neurorehabilitation. Curr. Opin. Neurobiol. 19 (1), 84–90. http://dx.doi.org/10.1097/01.wco.0000200544.29915.cc16415682.

Lehéricy, S., Gerardin, E., Poline, J.B., et al., 2004. Motor execution and imagination networks in post-stroke dystonia. Neuroreport 15 (12), 1887–1890. http://dx.doi.org/10.1097/00001756-200408260-0001015305130.

Li, J., Liu, J., Liang, J., et al., 2010. Effective connectivities of cortical regions for top-down face processing: a dynamic causal modeling study. Brain Res. 1340, 40–51. http://dx.doi.org/10.1016/j.brainres.2010.04.04420423709.

Li, S., Kamper, D.G., Stevens, J.A., et al., 2004. The effect of motor imagery on spinal segmental excitability. J. Neurosci. 24 (43), 9674–9680. http://dx.doi.org/10.1523/JNEUROSCI.2781-04.200415509755.

Livesay, J.R., Samaras, M.R., 1998. Covert neuromuscular activity of the dominant forearm during visualization of a motor task. Percept. Mot. Skills 86 (2), 371–374. http://dx.doi.org/10.2466/pms.1998.86.2.37110049098.

Luppino, G., Matelli, M., Camarda, R., et al., 1993. Corticocortical connections of area F3 (SMA-proper) and area F6 (pre-SMA) in the macaque monkey. J. Comp. Neurol. 338 (1), 114–140. http://dx.doi.org/10.1002/cne.9033801097507940.

Mazziotta, J.C., Toga, A.W., Evans, A., et al., 1995. A probabilistic atlas of the human brain: theory and rationale for its development. The International Consortium for Brain Mapping (ICBM). Neuroimage 2 (2), 89–101. http://dx.doi.org/10.1006/nimg.1995.10129434592.

McNeal, D.W., Darling, W.G., Ge, J., et al., 2010. Selective Long-term reorganization of the corticospinal projection from the supplementary motor cortex following recovery from lateral motor cortex injury. J. Comp. Neurol. 518 (5), 586–621. http://dx.doi.org/10.1002/cne.2221820034062.

Mintzopoulos, D., Astrakas, L.G., Khanicheh, A., et al., 2009. Connectivity alterations assessed by combining fMRI and MR-compatible hand robots in chronic stroke. Neuroimage 47, T90–T97. http://dx.doi.org/10.1016/j.neuroimage.2009.03.00719286464.

Mostany, R., Chowdhury, T.G., Johnston, D.G., et al., 2010. Local hemodynamics dictate long-term dendritic plasticity in peri-infarct cortex. J. Neurosci. 30 (42), 14116–14126. http://dx.doi.org/10.1523/JNEUROSCI.3908-10.201020962232.

Munzert, J., Lorey, B., Zentgraf, K., 2009. Cognitive motor processes: the role of motor imagery in the study of motor representations. Brain Res. Rev. 60 (2), 306–326. http://dx.doi.org/10.1016/j.brainresrev.2008.12.02419167426.

Nudo, R.J., Friel, K.M., Delia, S.W., 2000. Role of sensory deficits in motor impairments after injury to primary motor cortex. Neuropharmacology 39 (5), 733–742. http://dx.doi.org/10.1016/S0028-3908(99)00254-3.

Nudo, R.J., Milliken, G.W., Jenkins, W.M., et al., 1996. Use-dependent alterations of movement representations in primary motor cortex of adult squirrel monkeys. J. Neurosci. 16 (2), 785–8078551360.

Page, S.J., Levine, P., Leonard, A., 2007. Mental practice in chronic stroke: results of a randomized, placebo-controlled trial. Stroke 38 (4), 1293–1297. http://dx.doi.org/10.1161/01.STR.0000260205.67348.2b17332444.

Penny, W.D., Stephan, K.E., Daunizeau, J., et al., 2010. Comparing families of dynamic causal models. PLOS Comput. Biol. 6 (3). http://dx.doi.org/10.1371/journal.pcbi.100070920300649.

Penny, W.D., Stephan, K.E., Mechelli, A., et al., 2004. Comparing dynamic causal models. Neuroimage 22 (3), 1157–1172. http://dx.doi.org/10.1016/j.neuroimage.2004.03.02615219588.

Pool, E.M., Rehme, A.K., Fink, G.R., et al., 2013. Network dynamics engaged in the modulation of motor behavior in healthy subjects. Neuroimage 82, 68–76. http://dx.doi.org/10.1016/j.neuroimage.2013.05.12323747288.

Raffin, E., Mattout, J., Reilly, K.T., et al., 2012. Disentangling motor execution from motor imagery with the phantom limb. Brain 135 (2), 582–595. http://dx.doi.org/10.1093/brain/awr33722345089.

Rehme, A.K., Eickhoff, S.B., Grefkes, C., 2013. State-dependent differences between functional and effective connectivity of the human cortical motor system. Neuroimage 67, 237–246. http://dx.doi.org/10.1016/j.neuroimage.2012.11.02723201364.

Rigoux, L., Stephan, K.E., Friston, K.J., et al., 2014. Bayesian model selection for group studies — revisited. Neuroimage 84, 971–985. http://dx.doi.org/10.1016/j.neuroimage.2013.08.06524018303.

Rouiller, E.M., Babalian, A., Kazennikov, O., et al., 1994. Transcallosal connections of the distal forelimb representations of the primary and supplementary motor cortical areas in macaque monkeys. Exp. Brain Res. 102 (2), 227–243. http://dx.doi.org/10.1007/BF002275117705502.

Schaechter, J.D., Kraft, E., Hilliard, T.S., et al., 2002. Motor recovery and cortical reorganization after constraint-induced movement therapy in stroke patients: a preliminary study. Neurorehabilitation and Neural Repair 16 (4), 326–338. http://dx.doi.org/10.1177/154596830201600403.

Sharma, N., Baron, J.C., Rowe, J.B., 2009. Motor imagery after stroke: relating outcome to motor network connectivity. Ann. Neurol. 66 (5), 604–616. http://dx.doi.org/10.1002/ana.2181019938103.

Sharma, N., Pomeroy, V.M., Baron, J.C., 2006. Motor imagery: a backdoor to the motor system after stroke? Stroke 37 (7), 1941–1952. http://dx.doi.org/10.1161/01.STR.0000226902.43357.fc16741183.

Silasi, G., Murphy, T.H., 2014. Stroke and the connectome: how connectivity guides therapeutic intervention. Neuron 83 (6), 1354–1368. http://dx.doi.org/10.1016/j.neuron.2014.08.05225233317.

Solodkin, A., Hlustik, P., Chen, E.E., et al., 2004. Fine modulation in network activation during motor execution and motor imagery. Cereb. Cortex 14 (11), 1246–1255. http://dx.doi.org/10.1093/cercor/bhh08615166100.

Stephan, K.E., Penny, W.D., Daunizeau, J., et al., 2009. Bayesian model selection for group studies. Neuroimage 46 (4), 1004–1017. http://dx.doi.org/10.1016/j.neuroimage.2009.03.02519306932.

Stephan, K.E., Penny, W.D., Moran, R.J., et al., 2010. Ten simple rules for dynamic causal modeling. Neuroimage 49 (4), 3099–3109. http://dx.doi.org/10.1016/j.neuroimage.2009.11.01519914382.

Turken, A., Whitfield-Gabrieli, S., Bammer, R., et al., 2008. Cognitive processing speed and the structure of white matter pathways: convergent evidence from normal variation and lesion studies. Neuroimage 42 (2), 1032–1044. http://dx.doi.org/10.1016/j.neuroimage.2008.03.05718602840.

Uswatte, G., Taub, E., Morris, D., et al., 2006. The motor activity log-28: assessing daily use of the hemiparetic arm after stroke. Neurology 67 (7), 1189–1194. http://dx.doi.org/10.1212/01.wnl.0000238164.90657.c217030751.

Valdes-Sosa, P.A., Roebroeck, A., Daunizeau, J., et al., 2011. Effective connectivity: influence, causality and biophysical modeling. Neuroimage 58 (2), 339–361. http://dx.doi.org/10.1016/j.neuroimage.2011.03.05821477655.

Walsh, R.R., Small, S.L., Chen, E.E., et al., 2008. Network activation during bimanual movements in humans. Neuroimage 43 (3), 540–553. http://dx.doi.org/10.1016/j.neuroimage.2008.07.01918718872.

Wasserman, L., 2000. Bayesian model selection and model averaging. J. Math. Psychol. 44 (1), 92–107. http://dx.doi.org/10.1006/jmps.1999.127810733859.

Westlake, K.P., Nagarajan, S.S., 2011. Functional connectivity in relation to motor performance and recovery after stroke. Front. Syst. Neurosci. 5, 8. http://dx.doi.org/10.3389/fnsys.2011.0000821441991.

Wittenberg, G., Chen, R., Ishii, K., et al., 2003. Constraint-induced therapy in stroke: magnetic-stimulation motor maps and cerebral activation. Neurorehabil. Neural Repair 17 (1), 48–57.

Xu, L., Zhang, H., Hui, M., et al., 2013. Motor Execution and Imagination: A Comparison of Functional Connectivity Based on Connection Strength. Medical Imaging 2013: Biomedical Applications in Molecular, Structural, and Functional Imaging 8672. SPIE, Orlando, FL, United States.